RESEARCH ARTICLE

Direct synthesis of carbon nanotubes on fly ash particles to produce carbon nanotubes/fly ash composites

Fangxian LI[*], Cheng ZHOU, Pengfei YANG, Beihan WANG, Jie HU, Jiangxiong WEI, Qijun YU

School of Materials Science and Engineering, South China University of Technology, Guangzhou 510640, China
[*]*Corresponding author. E-mail: msfxli@scut.edu.cn*

ABSTRACT Fly ash was used as catalytic support for carbon nanotubes (CNTs) growth by chemical vapor deposition (CVD) due to having ideal compositions (SiO_2, Al_2O_3, and Fe_2O_3). In this paper, CNTs were synthesized on Ni catalyst/fly ash substrate using CVD method. The influence of parameters (e.g., reaction temperature and gas flow rate) on the carbon yield and structure of the resulting CNTs was on the carbon yield and structure of the resulting CNTs was investigated by thermo-gravimetric analyses, Scanning electron microscopy, and Raman spectroscopy analysis. The results indicated that the growth temperature controlling had a significant effect on the diameter of CNTs. And the proper acetylene and hydrogen flow rate would decrease in defect density and increase in yield of as-grown CNTs on fly ash. Finally, the amorphous carbon on the surface of as-grown CNTs were removed by heating in air. Experimental results showed that the hydrophobic of the annealed CNTs was weak due to introducing functional groups to the surface of CNTs.

KEYWORDS carbon nanotubes, fly ash, chemical vapor deposition, parameters, purification

1 Introduction

Carbon nanotubes (CNTs) were generally regarded as an optimal reinforcing materials for composites because of their nano-diameter, unique physical properties, superior strength, and toughness as well as excellent conductive properties [1–3]. Based on the excellent performance, using CNTs to enhance the mechanical, electrical, and thermal of composite materials has been pursued extensively and CNTs had been widely used in many engineering fields such as hydrogen storage [4], battery cathode composites [5], water treatment [6], electronic devices [7], and construction materials [8]. However, in order to take advantage of the CNTs excellent reinforcing efficiency, it was necessary to achieve a uniform distribution in the matrix because CNTs tend to agglomerate and form bundles. To solve the problem, researchers carried on a lot of studies and obtained some effective methods, such as surface chemical modification, dispersing by dispersant, ultrasonic dispersion, mechanical dispersion, dissolving in solution, and the combination of physical and chemical

methods [9,10]. As for cementitious composites, the above dispersion methods would present its own problems, for instance, poor bonding between CNTs and cementitious materials, unnecessary damaging to the mechanical properties of CNTs and negative effect on cement hydration.

Comparable to above methods, an optional machining approach to improve dispersion of CNT within cementitious substrate surfaces was to grow CNTs directly on the surface of substrate particles by *in situ* growth. The prepared CNTs hybrid material could use as an additive to cement-base mixture. Several methods have been developed to *in situ* growth of CNTs, including arc discharge method, microwave radiation method, laser ablation method, and chemical vapor deposition (CVD) method. Comparing with other methods, CVD is commonly used due to its low synthesis temperature, easy scale-up, cost effective, and prior success in producing uniform CNT growth on complex surfaces [2].

Nasibulin et al. [11] first employed CVD method to grow CNTs/CNFs on the surface of cement, in which cement with catalyst was heated to grow CNTs/CNFs in the carbon source gas environment. Mudimela et al. [12]

also tried CVD method to grow CNTs/CNFs on the surface of silica fume particles impregnated by iron salt. Furthermore, Ghaharpour et al. [13] also reported that CNTs were synthesized on Fe Catalyst/Portland cement substrate using CVD method, which could optimize the diameter and crystallinity of CNT by controlling the growth temperature. Ludvig et al. [14] also employed CVD method to grow CNTs/CNFs directly on the cement clicker and silica fume, but they added iron ore and industrial byproducts such as converter dust, steel mill scale and red mud as extra catalysts. Dunens et al. [15] employed the fluidized bed CVD method for *in situ* CNTs/CNFs growth on fly ash (FA) and included Fe content as a catalyst support similar to many laboratory-developed catalysts for CNTs/CNFs synthesis. Zhang et al. [2] reported the synthesis of multi-walled CNT on carbon fiber substrates with high density and uniform coverage via injection of a xylene-ferrocene solution into a CVD furnace.

During the CVD process, CNTs deposited on the surface of metal catalyst due to the thermal decomposition of hydrocarbon compounds (e.g., acetylene, methane, ethylene, benzene, etc.) at moderate temperatures (400°C–1100°C). According to above-mentioned researches, the morphologies, structures, dispersion, and interface of the resulting nanocarbon composites could be easily modulated by varying the experimental parameters (e.g., temperature, catalysts, carbon sources, gas flow rate, etc.), which enabled a great potential for the *in situ* synthesis of high-quality CNTs with tailored size and dimension for constructing high-performance composites [16]. Fly ash with broad size distribution contains SiO_2, Al_2O_3, Fe_2O_3, MgO, etc., catalytically materials for the growth of CNTs. Ratkovic et al. [17] found that alumina- and silica-supported using $Fe-Co/Al_2O_3$ as catalyst exhibited a high activity toward CNTs formation. Thereby, it could be directly used as catalytic substrate for the synthesis of CNTs. Furthermore, fly ash as catalytic substrate for CNT synthesis could provide a method toward utilizing the industrial byproduct of coal and biomass combustion. So far, there had been only a few published reports on fly ash being used as catalytic substrate for the synthesis of CNTs. The parameters in synthesizing CNTs with CVD method should be optimized in order to reach uniform distribution of CNTs accompanied by low amounts of amorphous carbon.

In this study, the application of fly ash as catalytic substrate for synthesis of CNTs in CVD method. A parametric study on the fly ash particles manufacturing process of CNTs was presented. The main aim of this paper was to investigate and understand the influence of growth parameters such as temperature, gas flow rate, and annealing in air on diameter of CNTs, CNTs morphology, and yield of carbon deposition. CNTs were deposited on fly ash using CVD with the utilization of Ni catalyst. The mass of the deposited material was measured by TG. Scanning electron microscopy (SEM) was used to visualize the surface of the fly ash after the CVD process. Raman spectroscopy was employed to analyze the structure defects of the as-grown CNTs.

2 Experimental

2.1 Materials

Fly ash, a main material, was used as a catalytic substrate for CNTs synthesis. The chemical compositions of fly ash determined by X-ray fluorescence (XRF) analysis were given in Table 1. Fly ash main components were SiO_2 and Al_2O_3, which were known to be appropriate support for the growth of CNTs [11,18].

2.2 Growth of CNTs

The synthesis of CNTs on the surface of fly ash particles was carried out in the experimental setup shown in Fig. 1(a). The reactor consisted of a quartz tube with diameter of 80 mm. First, to increase the content of catalyst in fly ash, the fly ash was soaked in 0.1 M ethanol-based nickel nitrate hexahydrate ($Ni(NO_3)_2 \cdot 6H_2O$) solution for 10 min according to the wet impregnation technique [19]. The mixture was stirred and heated at nearly 50°C until the alcohol evaporated completely. Acetylene was chosen as the main carbon source in this experiment. Figure 1(b) showed the process of the gas penetration for synthesis of CNTs. And all the gas was injected through a gas controller according to Table 2. At 450°C, the nitrogen (N_2) and hydrogen (H_2) gasses were introduced (N_2:H_2 = 400:400 mL/min) to reduce the catalyst for 60 min. Successively, the growth temperature for the CVD process was converted to desired temperature (e.g., 400°C, 500°C, 600°C, 700°C, 800°C). The CVD reaction would carry on for 45 min. Before the sample was removed, the tube and sample were cooled under flowing N_2 gas atmosphere to room temperature. The carbon yield calculated by Eq. (1):

$$\text{Carbon yeild} = \frac{M_{\text{total}} - M_{\text{f}}}{M_{\text{total}}} \times 100\%, \quad (1)$$

where M_{total} was the total mass of carbon product and fly ash, and M_{f} was the mass of fly ash.

Table 1 Metal oxide concentration and oxide stoichiometry ratios of fly ash determined by XRF.

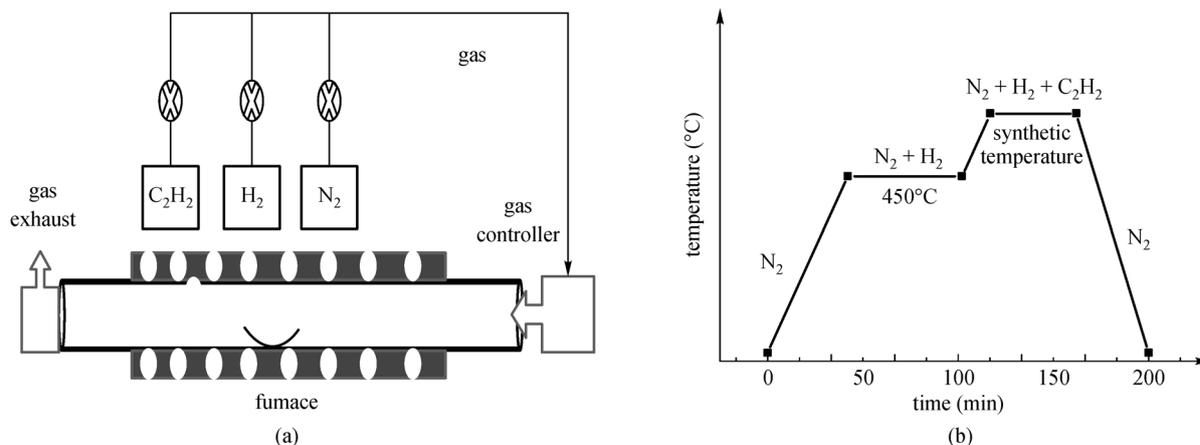| component	SiO$_2$	CaO	Al$_2$O$_3$	Fe$_2$O$_3$	Cr$_2$O$_3$	K$_2$O	MgO	SO$_3$	TiO$_2$	NaO$_2$	P$_2$O$_5$	loss
content (wt%)	52.55	6.98	29.80	4.67	0.08	1.34	1.00	0.93	1.01	0.66	0.39	0.59

Fig. 1 (a) Schematic representation of the experimental device and (b) process of the gas penetration for synthesis of CNTs.

Table 2 Different flow rate of the supply gas for CNTs synthesis.

groups	C_2H_2 (mL/min)	H_2 (mL/min)	N_2 (mL/min)
A1	100	400	800
A2	200	400	800
A3	400	400	800
B1	200	0	800
B2	200	200	800
B3	200	400	800
B4	200	600	800

2.3 Characterization

In this work, the synthesized CNTs was characterized by X-ray diffraction (XRD), thermo-gravimetric analyses (TG), SEM, and Raman spectrum. XRD patterns were obtained in a rotation anode X-ray diffractometer (PANalytical, Netherlands) by using Cu-Kα radiation. And diffraction angle were recorded in a 2θ range from 5° to 90° at a scan speed of 10°/min. SEM (Zeiss, Germany) was also performed at an operating voltage of 10 kV for the investigation of the morphology of CNTs /fly ash composites. TG was conducted in air at a rate of 100 mL/min. The thermos program was between 50°C and 900°C with a heating rate of 10°C/min. Raman spectra was recorded in a range of 800–3000 cm^{-1}. The CNTs showed two strong peaks near 1320 and 1590 cm^{-1}, corresponding to the D- and G-bands, respectively, whereas the D-band was associated with the disorder features of the hexagonal graphitic layers [20]. G-band was attributed to the stretching vibration of carbon sp^2 bonds in a hexagonal lattice [21]. The I_D/I_G ratios was obtained by calculating the intensity ratio of D-band to G-band, which was generally used as a characteristic of nanotube quality.

3 Results and discussion

There were several variable parameters in the CVD process that might affect the synthesis of CNT, including type of catalyzer, the flow rate of gas, and synthesis temperature. To determine the relative influence of CVD growth conditions on the morphology and structure of the CNTs/fly ash composites, temperature and gas flow rate were varied.

3.1 Synthesis of CNTs on the fly ash by CVD

To verify the growth of CNTs on fly ash particles, the synthesis temperature was set at 500°C, and the flow rate of acetylene was set 400 mL/min. Figure 2 showed the XRD patterns for fly ash (FA) before and after CVD reaction, respectively. Peaks of silicon oxide and mullite could be found in the XRD patterns. Comparing to the pristine fly ash, the intensity of the diffraction peak at 26.5° corresponding to the graphite-like phase for fly ash after
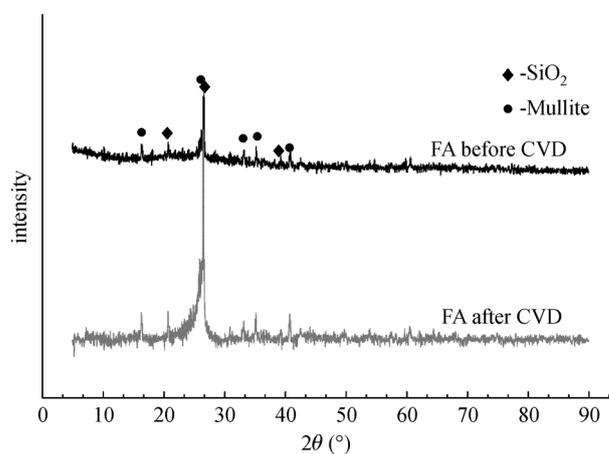

Fig. 2 XRD spectra of fly ash (FA) before and after CVD.

the CVD process was more predominant. An average inter-layer distance (0.34 nm) for the carbon following from Bragg's law could be calculated, which was due to the graphitization of CNTs grown on fly ash particles [17]. This was confirmed by the SEM image of fly ash before and after CVD reaction. Figure 3 indicated that the surface of fly ash was covered with randomly oriented and compact CNTs, which confirmed that fly ash as a substrate was beneficial to the growth of CNTs.

3.2 The effect of CNT growth temperature

To investigate the influence of growth temperature on the yield and structure of as-grown CNTs synthetized on the fly ash by CVD, the experiments were conducted at five different temperature values (400°C, 500°C, 600°C, 700°C, and 800°C). Acetylene with a flow rate of 400 mL/min accompanied by N_2 and H_2 were passed through the catalytic substrate for 45 min. Due to the high thermal stability of fly ash, the yield and the thermal stability of

CNTs could be effectively characterized by TGA. The results are shown in Fig. 4 and Table 3. It could be observed that there was a stepwise weight losses on the trace of the TG curve (see Fig. 4(a)), which was assigned to the oxidation of amorphous carbon and CNTs according to literature report. The initial oxidation temperatures of the synthesized CNTs were significant difference at different synthesis temperatures. And the weight loss of CNTs/fly ash composites increased by 54wt% at 600°C (see Fig. 4(b)). However, there was a lower yield of as-grown CNTs at 400°C and 800°C. It was demonstrated that the temperature had a significant effect on the yield of carbon deposition [22]. The reason might be assigned to the activity of catalyst speeding up acetylene decomposition at 600°C. The suitable temperature (600°C) would stimulate the degradation of acetylene which as a result raised the growth rate and abundance of CNTs. Highly crystalline CNTs were more resistant to oxidation, which made them more stable under a higher temperature. The thermal stability was directly attributed to the aromatic bonding
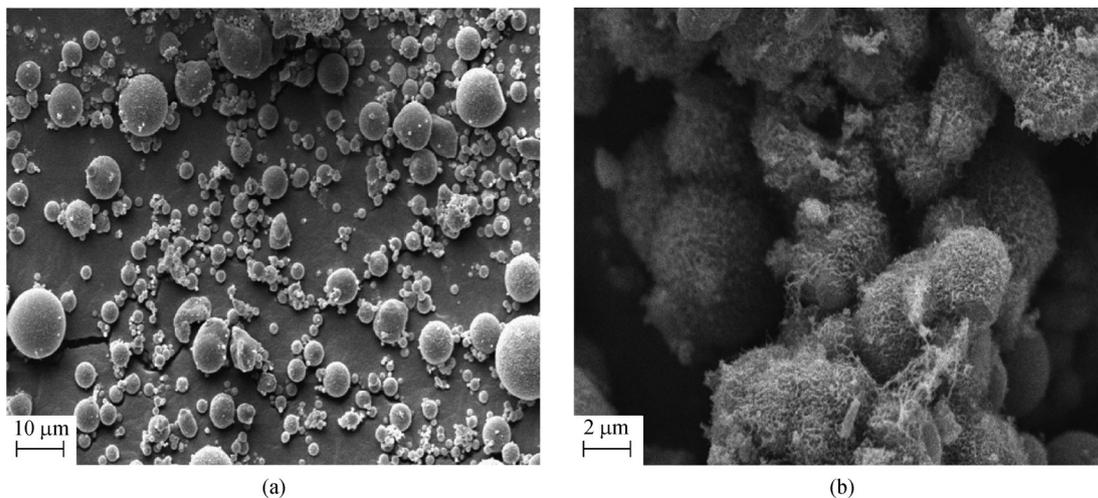

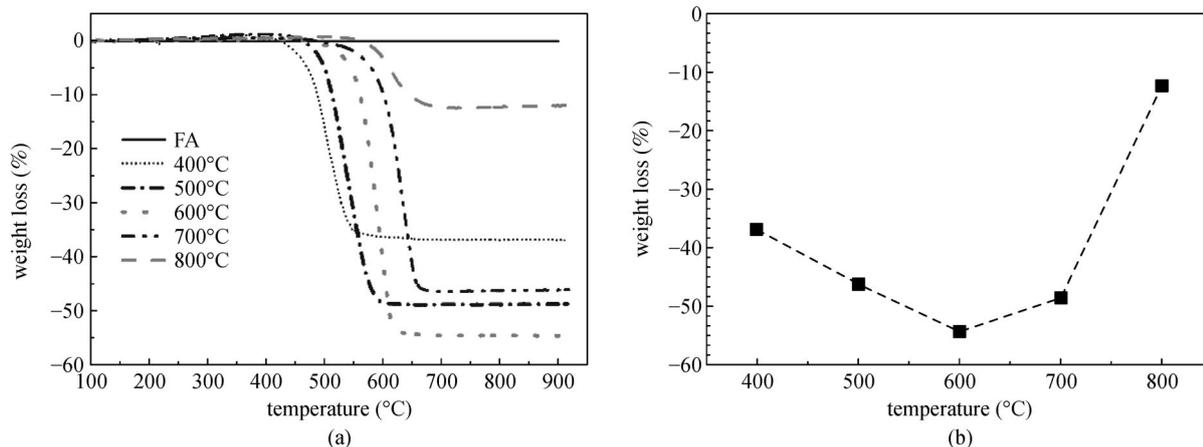**Fig. 3** SEM images of fly ash (a) before and (b) after CVD reaction.

Fig. 4 Effect of temperature on the yield and thermal stability of CNTs. (a) TGA profiles; (b) effect of temperature on the weight loss.

within the CNT structure, including the number of walls, the presence and composition of catalyst, the defects within the tubes, and the presence of other materials within the sample (i.e., amorphous carbon, graphitic particles) [23]. Table 3 summarized the onset and the end temperatures of CNTs/fly ash composites, at which represented the initial and the final weight loss, respectively took place. And the smaller difference between the onset and end temperature imply better graphitized CNTs [24]. These results indicated that the onset oxidation temperature of the CNTs/fly ash composites was related to synthesis temperature, where the onset oxidation temperature increased with the increase of growth temperature. However, in the process of CVD, the production of amorphous carbon was inevitable, which also affected the thermal stability of CNTs. In case of the CNTs synthetized

at 700°C, a large difference (189°C) between the onset and end temperatures indicated a low graphitized structure of CNTs (Table 3). It was due to the formation of the more amorphous carbon and structural defects in CNTs/fly ash composites [24].

The morphology of the CNTs/fly ash composites at the temperatures of 500°C, 600°C, and 700°C were shown in Fig. 5. As seen from the images, fly ash particles were completely covered by carbon nanomaterials. On the surface of fly ash particles, mainly CNTs with the diameters varied from 20 to 50 nm were observed at 500°C. As the growth temperature increased, the diameter of CNTs gradually increased. The diameter of CNTs varied from 70 to 140 nm at 600°C and from 200 to 300 nm at 700°C. Due to the probability of catalyst atoms agglomeration at a high temperature, hydrocarbon gas decomposition rate increased and more carbon atoms were accessible for growing CNTs with thicker walls [13]. Therefore, the diameter of CNTs synthesized at a high temperature increased, resulting in a high antioxidant capacity [25].

To further investigate the structure, crystallinity and graphitization degree of the as-grown CNTs on fly ash particles, Raman spectroscopic measurements was carried out to check the homogeneity of the crystalline phases present in the sample. The basis of the I_D/I_G ratio was

Table 3 TGA data of the FA/CNTs synthesized at different temperature.

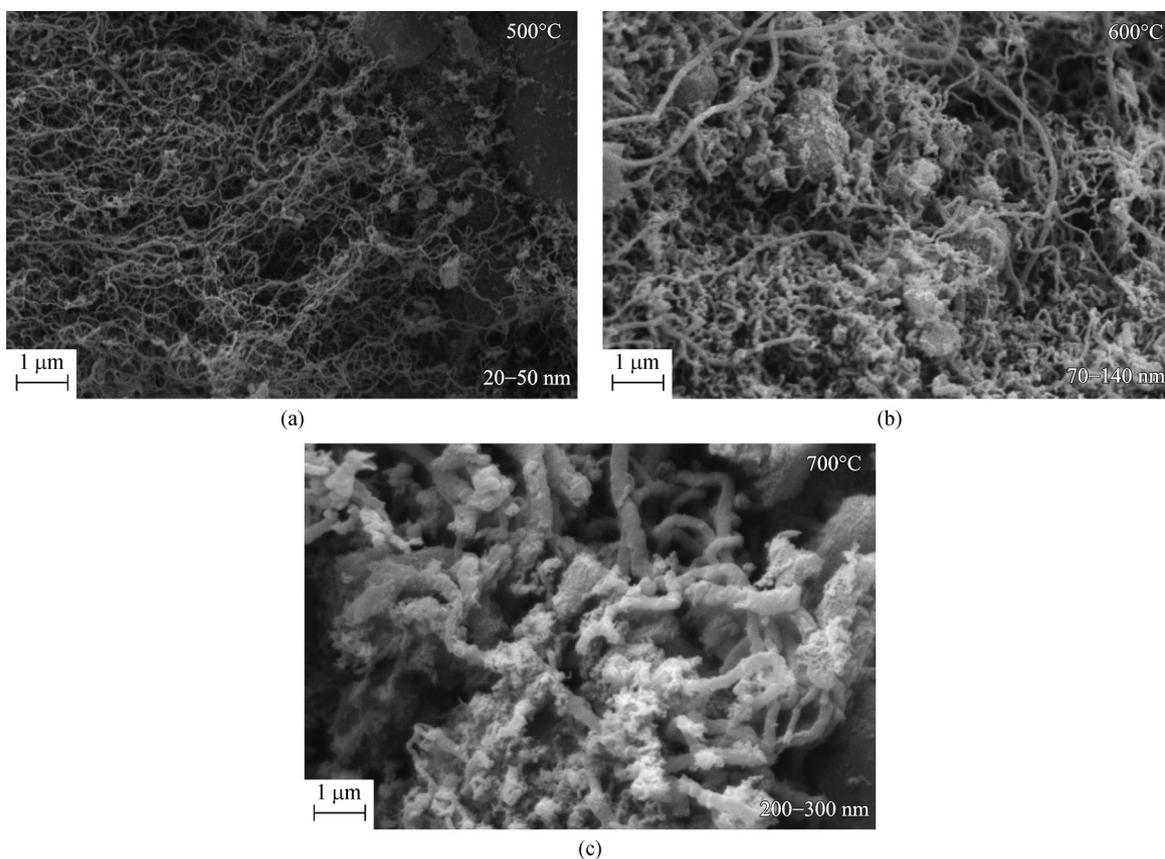| temperature (°C)	onset temperature (°C)	end temperature (°C)	difference (°C)
400	422	568	146
500	459	692	143
600	470	631	161
700	480	669	189
800	561	684	123

Fig. 5 SEM images of CNTs synthesized on fly ash particles at different synthesis temperature. (a) 500°C; (b) 600°C; (c) 700°C.

frequently used as a reliable parameter to assess the degree of disorder and defect content in carbon materials. Figure 6 displayed that the I_D/I_G ratio of the as-grown CNTs reached the maximum (1.79) at 700°C, which indicated that the CNTs grown at 700°C were more defective and in a lower crystallinity degree compared to those grown at other temperatures [26]. These results were similar with the report in previous studies where Fe-supported catalysts were used [27].
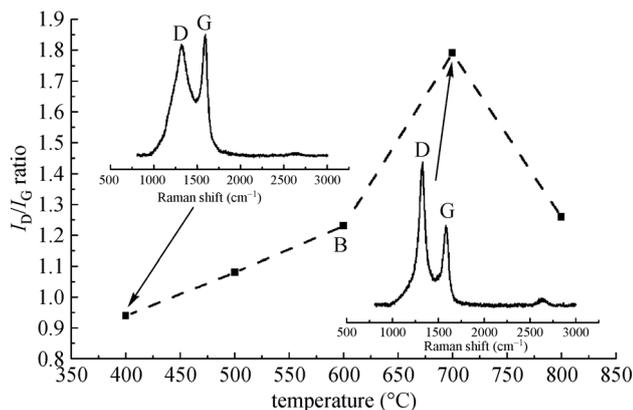

Fig. 6 The I_D/I_G ratio of CNTs grown on fly ash at different temperatures.

3.3 The effect of gas flow rate

3.3.1 Acetylene

Figure 7 showed a significant difference in the yield of CNTs synthesized under different acetylene flow rate. The yield increased with the increase of the acetylene flow rate. It implied that an increase in precursor gas flow increased the availability of reactants resulting in increased carbon deposition which was also reported in Ref. [28]. The flow

rate of the acetylene might affect the structural character-istics of the CNTs. Figure 7(b) showed a low I_D/I_G ratio of as-grown CNTs when acetylene flow rate was 200 mL/min, suggesting the less defective tubes in the as-grown CNTs compared to that synthetized at acetylene gas flow rate of 100 and 400 mL/min. SEM images of the samples synthesized at different acetylene gas flow rate were shown in Fig. 8. There was a significant difference in the mass of the CNTs over the surface of fly ash particles and the diameter of CNTs did not change significantly when the flow rate of acetylene increased, which was consistent with the results of thermo-gravimetric analyses.

3.3.2 Hydrogen

To better understand the effect of hydrogen flow rate on the CNT crystallinity, the hydrogen flow rate ranged from 0 to 600 mL/min. Figure 9 showed that the carbon yield of CNTs/fly ash composites increased with the increase of the hydrogen flow rate. In terms of CNTs yield, hydrogen contributed to a higher yield. Yardimci et al. [29] also reported that the hydrogen atmosphere could accelerate the growth of CNTs. Raman spectrum of the I_D/I_G ratio of the CNTs/fly ash composites in different hydrogen flow rate were given in Fig. 9. For hydrogen flow rates ranging from 0 to 400 mL/min, the defect density of CNTs decreased with the increase of the hydrogen content. At relatively low flow rates, hydrogen could help etching CNTs, hence increasing the I_D/I_G ratio. And at a high flow rate, the adsorption of hydrogen on the defect sites resulted in the occurrence of structural transformations in the continuous cylindrical graphene walls of CNTs [21]. When the flow rate was 600 mL/min, the I_D/I_G ratio increased by 1.38.

3.4 Purification of CNTs

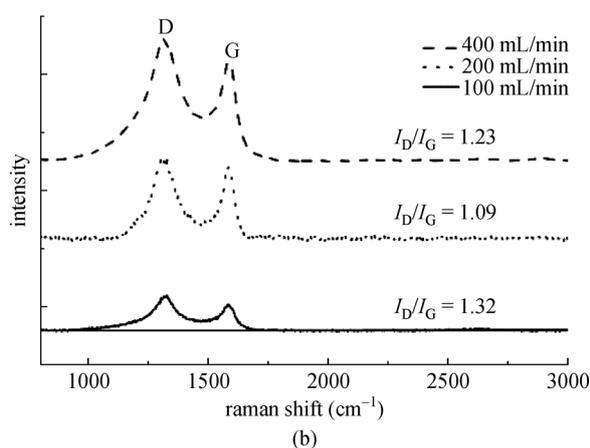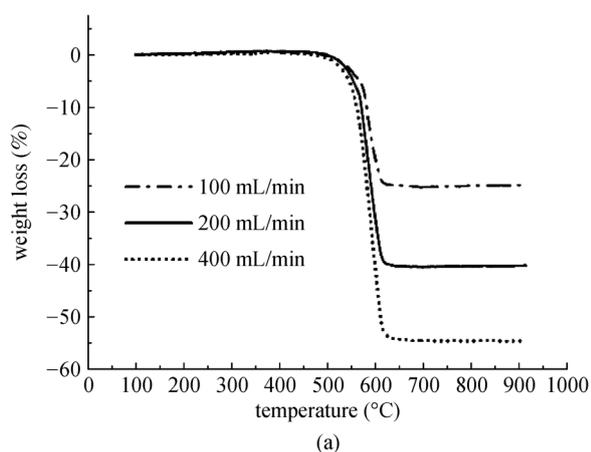Figure 10 showed the water droplets on fly ash and CNTs/

Fig. 7 TGA profiles and Raman spectra for CNTs synthesized on fly ash particles with different C_2H_2 flow rate. (a) TGA profiles; (b) Raman spectra.
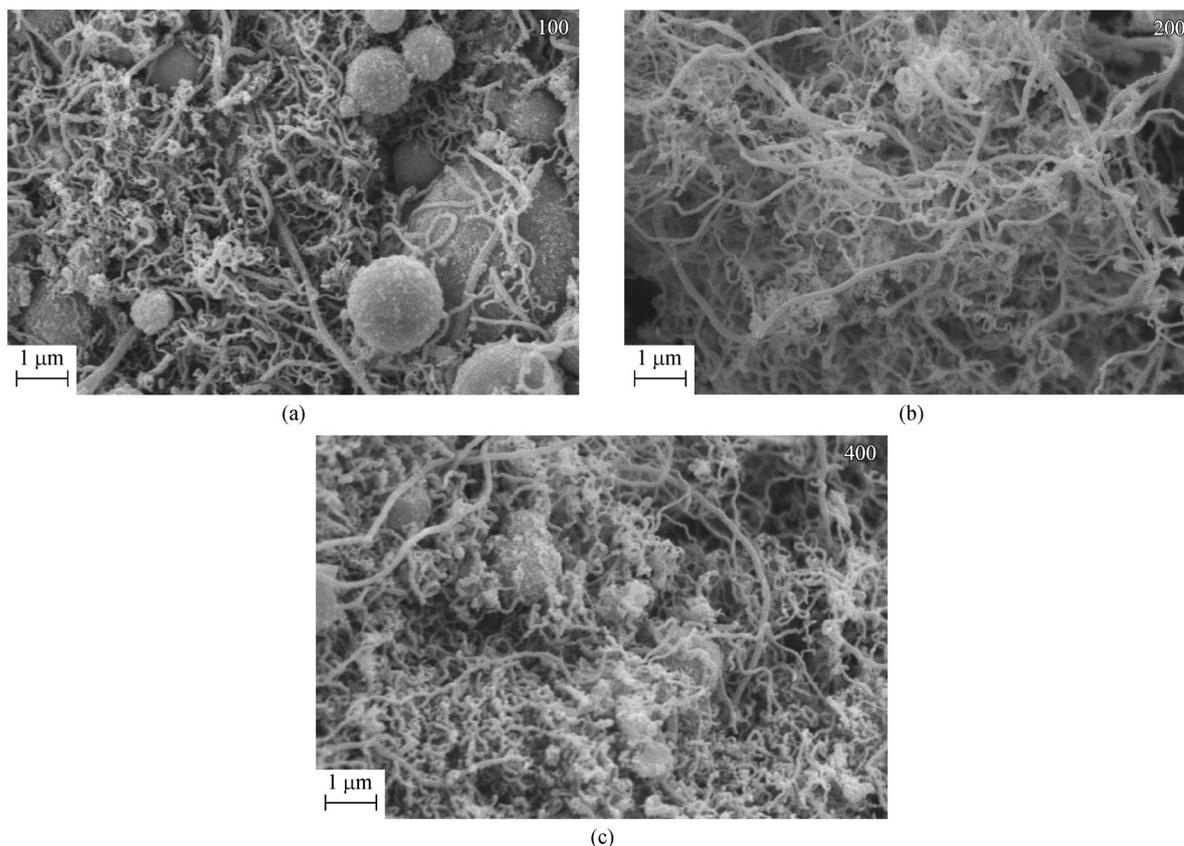
Fig. 8 SEM images of CNTs synthesized on fly ash particles with different C_2H_2 flow for furnace temperature of 600°C. (a) 100 mL/min; (b) 200 mL/min; (c) 400 mL/min.
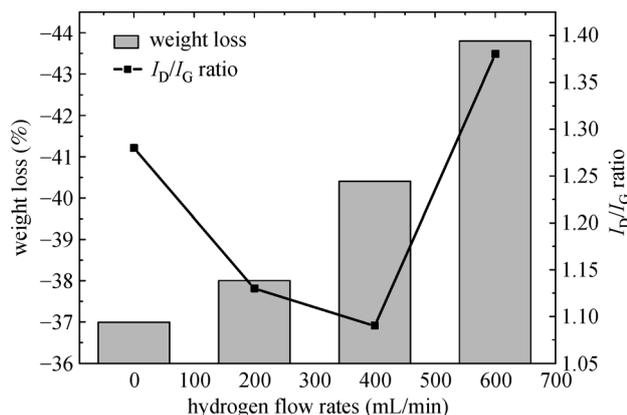

Fig. 9 Effect of hydrogen flow rate on the yield and I_G/I_D ratio.

fly ash templates, respectively. It confirmed that the as-grown CNTs on the fly ash particles made them moderately hydrophobic. Due to the fact that the pristine CNTs annealed in the air could remove impurity on the surface of the CNTs [30], the CNTs/fly ash composites were annealed in air for purification. Figure 11(a) showed the water contact angle of fly ash/CNTs composites and fly ash/CNTs composites heated at 300°C for 2 h. The hydrophobic of the fly ash/CNTs composites obviously

weakened after heated for 2 h. The results observed by Raman spectra confirmed that the I_D/I_G ratio of the fly ash/CNTs composites heated in air was lower than the fly ash/CNTs composites in Fig. 11(b), indicating less defect in the purified CNTs. It was attributed to the oxidation of amorphous carbon on the surface of the as-grown CNTs [31,32].

XPS analysis provided further characterization of the purified CNTs. Figure 12 showed the C1s XPS spectrum of as-grown CNTs and the purified CNTs at different temperatures, respectively. To analyze the chemical bonds of functional groups, the C 1s spectra was deconvoluted into four component peaks. All spectra had a major peak around 284.5 eV corresponding to C–C/C = C bonds, and smaller peaks associated with such oxygen containing bonds as C–O (around 285.7 eV), C = O (around 287.1 eV), and O–C = O (around 288.9 eV) [33,34].

The concentrations of the corresponding functional groups were summarized in Table 4. The carbon atom percent of C–C/C = C changed from 92.5% for control to 75% for purified CNTs. And carboxylic acid on surface of the CNT was proved by the increase of intensity for C = O peak at 287.1 eV and the appearance of the peak of O–C = O at 288.9 eV. The hydrophobicity of purified fly
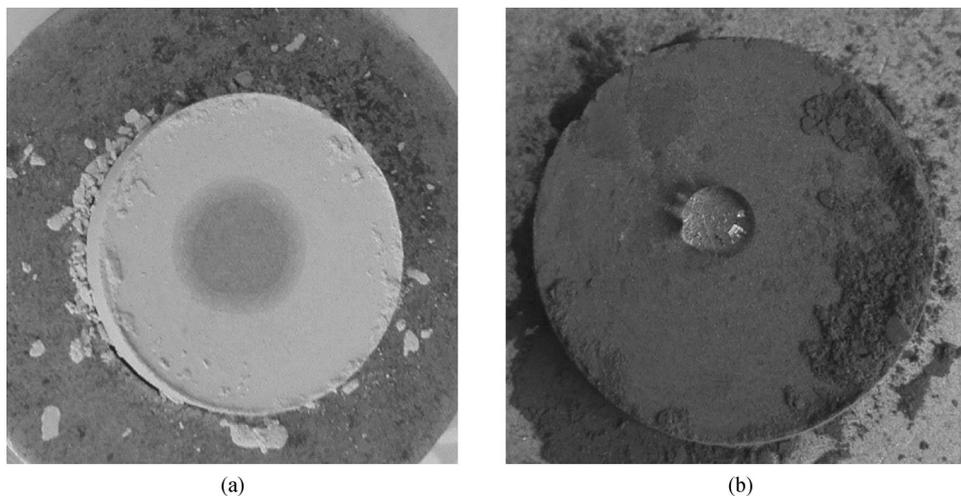
Fig. 10 Photographs of water droplet shape on (a) fly ash template and (b) fly ash/CNTs template with the conventional pressing plate method.
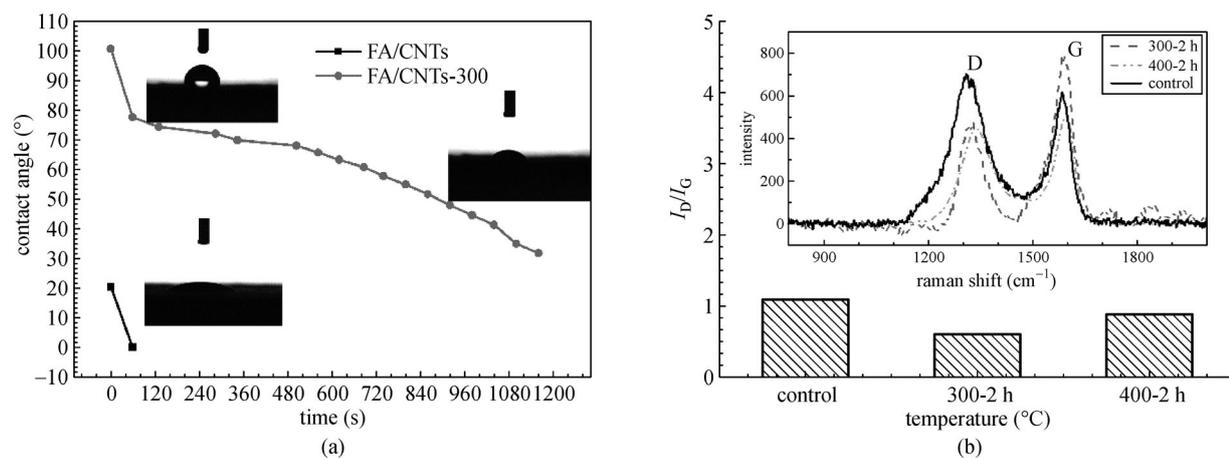

Fig. 11 Effect of purification on CNTs/fly ash templates. (a) Water contact angle for fly ash/CNT composite and fly ash/CNTs composites heated at 300°C for 2 h; (b) the I_G/I_D ratio of fly ash/ CNTs composite and fly ash/CNTs composite heated in air at 300°C, 400°C for 2 h.

ash/CNTs composite weakened due to the introduce of these functional groups, which suggested that the method by annealing in air could effective remove the impurities and introduce functional groups on the surface of CNTs.

4   Conclusions

CNTs were synthesized on Ni catalyst supported fly ash particles by CVD method and the influence of growth parameters on the yield and quality of CNTs were investigated. The experimental results showed that:

1) CNTs could be synthesized on the fly ash substrate at a low temperature (400°C). The diameter of CNTs increased with the increase of the temperature. The yield of CNTs increased with the increase of temperature lower than 600°C, and then decreased with the temperature increases. However, the defect density in CNTs at 700°C were highest indicating the most structural defects in CNTs/fly ash composites

2) The yield of CNTs increased with the increase of the flow rate of acetylene or hydrogen. The CNTs synthetized at acetylene gas flow rate of 200 mL/min and hydrogen gas flow rate of 400 mL/min had less defective density. It can be concluded that the gas flow rate for $C_2H_2:H_2:N_2 = 200:400:800$ mL/min was a suitable condition for synthesizing CNTs on fly ash particles.

3) The amorphous carbon in the surface layer of CNTs would be removed by heating at 300°C for 2 h in the air. The hydrophobicity of fly ash/CNTs composites decreased due to the produce of oxygen functional groups on the surface of CNTs.
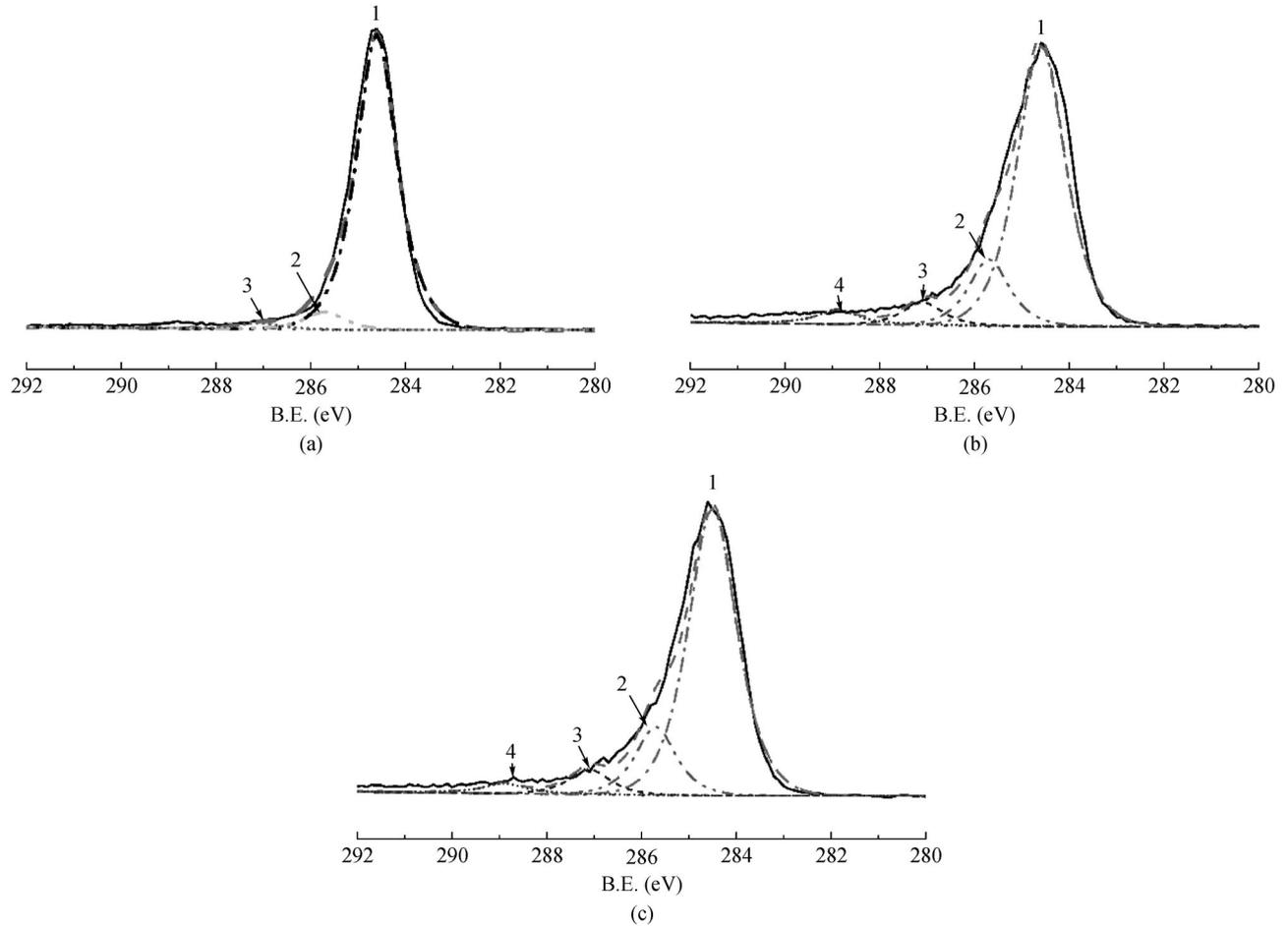
Fig. 12 XPS C 1s spectra of (a) raw fly ash/CNTs; (b) fly ash/CNTs heated in air at 300°C for 2 h; (c) fly ash/CNTs heated in air at 400°C for 2 h (1: C–C/C = C; 2: –C–O; 3: –C = O; 4: –COOH (–COO)).

Table 4 Quantitative analysis derived from XPS.

sample	C–C/C = C	–C–O	–C = O	–COO
fly ash/CNTs	92.5%	5.5%	2.0%	–
purified fly ash/CNTs at 300°C	75.0%	15.4%	5.3%	4.3%
purified fly ash/CNTs at 400°C	74.5%	15.4%	5.7%	4.4%

References

1. Kim H K, Nam I W, Lee H K. Enhanced effect of carbon nanotube on mechanical and electrical properties of cement composites by incorporation of silica fume. Composite Structures, 2014, 107: 60–69

2. Zhang Q, Liu J, Sager R, Dai L, Baur J. Hierarchical composites of carbon nanotubes on carbon fiber: Influence of growth condition on fiber tensile properties. Composites Science and Technology, 2009, 69(5): 594–601

3. Khalili S, Haghbin A. Investigation on design parameters of single-walled carbon nanotube reinforced nanocomposites under impact loads. Composite Structures, 2013, 98: 253–260

4. Yang Z, Xia A Y, Mokaya R. Enhanced hydrogen storage capacity of high surface area zeolite-like carbon materials. Journal of the American Chemical Society, 2007, 129(6): 1673–1679

5. Hagen M, Dörfler S, Althues H, Tübke J, Hoffmann M J, Kaskel S, Pinkwart K. Lithium-sulphur batteries—Binder free carbon nanotubes electrode examined with various electrolytes. Journal of Power Sources, 2012, 213: 239–248

6. Lu C, Chung Y L, Chang K F. Adsorption of trihalomethanes from water with carbon nanotubes. Water Research, 2005, 39(6): 1183–

1189

7. Schnorr J M, Swager T M. Emerging applications of carbon nanotubes. Chemistry of Materials, 2011, 23(3): 646–657

8. Chaipanich A, Nochaiya T, Wongkeo W, Torkittikul P. Compressive strength and microstructure of carbon nanotubes-fly ash cement composites. Materials Science and Engineering A-Structural Materials Properties Microstructure and Processing, 2010, 527(4–5): 1063–1067

9. Sun S, Yu X, Han B, Ou J. *In situ* growth of carbon nanotubes/carbon nanofibers on cement/mineral admixture particles: A review. Construction & Building Materials, 2013, 49: 835–840

10. Raki L, Beaudoin J, Alizadeh R, Makar J, Sato T. Cement and concrete nanoscience and nanotechnology. Materials (Basel), 2010, 3(2): 918–942

11. Nasibulin A G, Shandakov S D, Nasibulina L I, Cwirzen A, Mudimela P R, Habermehl-Cwirzen K, Grishin D A, Gavrilov Y V, Malm J E M, Tapper U, Tian Y, Penttala V, Karppinen M J, Kauppinen E I. A novel cement-based hybrid material. New Journal of Physics, 2009, 11(2): 023013

12. Mudimela P R, Nasibulina L I, Nasibulin A G, Cwirzen A, Valkeapaa M, Habermehl-Cwirzen K, Malm J E M, Karppinen M J, Penttala V, Koltsova T S, Tolochko O V, Kauppinen E I. Synthesis of carbon nanotubes and nanofibers on silica and cement matrix materials. Journal of Nanomaterials, 2009, 2009: 1–4

13. Ghaharpour F, Bahari A, Abbasi M, Ashkarran A A. Parametric investigation of CNT deposition on cement by CVD process. Construction & Building Materials, 2016, 113: 523–535

14. Ludvig P, Calixto J M, Ladeira L O, Gaspar I C P. Using converter dust to produce low cost cementitious composites by *in situ* carbon nanotube and nanofiber synthesis. Materials (Basel), 2011, 4(3): 575–584

15. Dunens O M, Mackenzie K J, Harris A T. Synthesis of multiwalled carbon nanotubes on fly ash derived catalysts. Environmental Science & Technology, 2016, 113: 523–535

16. He C, Zhao N, Shi C, Liu E, Li J. Fabrication of nanocarbon composites using *in situ* chemical vapor deposition and their applications. Advanced Materials, 2015, 27(36): 5422–5431

17. Ratkovic S, Peica N, Thomsen C, Bukur D B, Boskovic G. Thermal stability evolution of carbon nanotubes caused by liquid oxidation. Journal of Thermal Analysis and Calorimetry, 2014, 115(2): 1477–1486

18. Metaxa Z S, Konsta-Gdoutos M S, Shah S P. Carbon nanofiber cementitious composites: Effect of debulking procedure on dispersion and reinforcing efficiency. Cement and Concrete Composites, 2013, 36: 25–32

19. Kashi M B, Aghababazadeh R, Arabi H, Mirhabibi A. Synthesis of high-quality single- and double-walled carbon nanotubes on Fe/MgO catalysts. Nanomaterials and Nanotechnology, 2016, 6: 381–389

20. Allaedini G, Tasirin S M, Aminayi P. Synthesis of CNTs via chemical vapor deposition of carbon dioxide as a carbon source in the presence of NiMgO. Journal of Alloys and Compounds, 2015, 647: 809–814

21. Ma Y, Dichiara A B, He D, Zimmer L, Bai J. Control of product nature and morphology by adjusting the hydrogen content in a continuous chemical vapor deposition process for carbon nanotube synthesis. Carbon, 2016, 107: 171–179

22. Allaedini G, Tasirin S M, Aminayi P. Yield optimization of nanocarbons prepared via chemical vapor decomposition of carbon dioxide using response surface methodology. Diamond and Related Materials, 2016, 66: 196–205

23. Lehman J H, Terrones M, Mansfield E, Hurst K E, Meunier V. Evaluating the characteristics of multiwall carbon nanotubes. Carbon, 2011, 49(8): 2581–2602

24. Awadallah A E, Aboul-Enein A A, Aboul-Gheit A K. Effect of progressive Co loading on commercial Co-Mo/Al$_2$O$_3$ catalyst for natural gas decomposition to CO$_x$-free hydrogen production and carbon nanotubes. Energy Conversion and Management, 2014, 77: 143–151

25. Zhang X, Zhang Q, Zheng J. Effect and mechanism of iron oxide modified carbon nanotubes on thermal oxidative stability of silicone rubber. Composites Science and Technology, 2014, 99: 1–7

26. Munir K S, Qian M, Li Y, Oldfield D T, Kingshott P, Zhu D M, Wen C. Quantitative analyses of MWCNT-Ti powder mixtures using raman spectroscopy: The influence of milling parameters on nanostructural evolution. Advanced Engineering Materials, 2015, 17(11): 1660–1669

27. Hintsho N, Shaikjee A, Masenda H, Naidoo D, Billing D, Franklyn P, Durbach S. Direct synthesis of carbon nanofibers from South African coal fly ash. Nanoscale Research Letters, 2014, 9(1): 387–398

28. Golshadi M, Maita J, Lanza D, Zeiger M, Presser V, Schrlau M G. Effects of synthesis parameters on carbon nanotubes manufactured by template-based chemical vapor deposition. Carbon, 2014, 80: 28–39

29. Yardimci A I, Yılmaz S, Selamet Y. The effects of catalyst pretreatment, growth atmosphere and temperature on carbon nanotube synthesis using Co-Mo/MgO catalyst. Diamond and Related Materials, 2015, 60: 81–86

30. Cao A, Liu G, Wang L, Liu J, Yue Y, Zhang L, Liu Y. Growing layered double hydroxides on CNTs and their catalytic performance for higher alcohol synthesis from syngas. Journal of Materials Science, 2016, 51(11): 5216–5231

31. Dementev N, Osswald S, Gogotsi Y, Borguet E. Purification of carbon nanotubes by dynamic oxidation in air. Journal of Materials Chemistry, 2009, 19(42): 7904–7908

32. 32.Naseh M V, Khodadadi A A, Mortazavi Y, Pourfayaz F, Alizadeh O, Maghrebi M. Fast and clean functionalization of carbon nanotubes by dielectric barrier discharge plasma in air compared to acid treatment. Carbon, 2010, 48(5): 1369–1379

33. Kuzmenko V, Naboka O, Haque M, Staaf H, Göransson G, Gatenholm P, Enoksson P. Sustainable carbon nanofibers/nanotubes composites from cellulose as electrodes for supercapacitors. Energy, 2015, 90: 1490–1496

34. Im Y O, Lee S H, Kim T, Park J, Lee J, Lee K H. Utilization of carboxylic functional groups generated during purification of carbon nanotube fiber for its strength improvement. Applied Surface Science, 2017, 392: 342–349